



VIVWPGEN (Vortex Induced Vibration Wind Power Generation): A Device to Harvest Wind Energy using Wind Blow Induced Vibration

Anand Prakash Pandey¹, Manju Bhardwaj², Akash Jaiwal³, Rohit Singh⁴, Prashant Baredar⁵

^{1,2,4}(FoEEE, Sri Ramswaroop Memorial University, Lucknow-Deva Road, Barabanki, UP, India)

³(DOECE, Roorkee Institute of Technology, Roorkee, Uttarakhand, India)

⁵(Dept. of Energy, Maulana Azad National Institute of Technology, Bhopal, MP, India)

Abstract- To fulfil the ever increasing energy demand, thus increased fossil fuels consumption globally has been posing the serious concern of global warming and climate change. This has shifted focus of research on renewable, eco-friendly green sources of energies. Geophysical fluid flows (wind/river/ocean) are readily available potential sources of clean, sustainable and renewable energy, worthwhile to meet up to large extent the world energy demand by means of e.g. wind turbines, hydro turbines, marine turbines and wave energy converters, etc. Since geophysical fluid flows have low energy density, therefore large power generation systems are needed to harness the optimum energy. A device intended to harness the energy from geophysical flows must have high energy density, be robust, be unobtrusive, has low maintenance and has a 10–20 years of operational life.

The energy converter systems using vortex induced vibration can fulfil all these criteria. VIV is the fluid-structure interaction phenomenon in which a non-streamlined body called bluff body, submerged in the flowing fluid causes alternate formation and shedding of vortices behind it downstream the flow. The vortex shedding exerts alternating lift force perpendicular to the direction of flow on the body and the body sets in oscillatory motion. In general, VIV is destructive to the vibrating structures such as high rise buildings, offshore mechanical and civil structures, and care should be exercised to reduce it by optimum design to prevent failure of the system. However, in energy harvesting using VIV, instead of spoiling vortex shedding, VIVs are exploited to increase the amplitude of vibrations, and this vibrational kinetic energy is converted into electric energy.

Based on the literature and the past research, we did an initial mathematical model calculation to establish feasibility of small scale VIVWPGEN and to predict the effect of



various parameters on the performance of its physical prototype. We have built a prototype of VIVWPGEN, and measurement results are compared with mathematical model analysis and conclusions are presented. Additionally examined and explored are the impacts of "lock in" phenomena and the surface geometry of bluff bodies (vibrators) on energy conversion efficiency. In order to achieve the best energy conversion efficiency, the design scalability for various aspect ratios of the VIVWPGEN vibrator is also investigated.

Keywords— Bluff bodies, Vortex Induced Vibration, Vortex Shedding, Lock in, Renewable Energy, Green Tech.

1.0. Introduction

A turbine generator (hydro or wind) is a mature technology however as size their increases so the frictional losses in the gear assembly and bearings also increase leading to decrease in efficiency of power conversion. Also, they require huge operating and maintenance cost because of the fatigue, wearing and tearing of rotating parts, blades etc. [1, 8]. The energy harvesting from vibration induced by flowing fluid is a promising new technology under research which can overcome these problems. There are three main types: the energy harnessing system from vortex-induced vibration (VIV) of bluff bodies, the flutter energy harvesting systems and the energy harvesting system with Helmholtz resonators [1]. Out of these the energy harvesting from VIV is more promising due to its salient features viz. less initial capital investment, do not pose any serious threat to eco-system and are scalable and versatile as they can be used to harvest energy from water bodies and/or rivers, Gulf Stream and wind blow [1-5]. A VIV based energy harvester can harness energy with high ratio of power conversion even in slow moving waterways (slow down to 0.25 m/s) over a wide range of frequency of vortex shedding by incorporating optimal damping. Usually, the phenomena of VIVs are observed over a broad range of Reynolds number except for three transition zones where they are suppressed.

The VIV based hydrokinetic energy converters concept to harness water kinetic energy was developed by various researchers especially the aquatic energy harvesting system (the VIVACE) by M. Bernitsas. Using air as flow medium poses some difficulties as air density is less about 1000 times than the water, which produces small lift forces not able to induce motion if weight of the oscillating system is too large. However, the potential of wind energy harvesting through VIVs would be more beneficial. This idea of expansion has motivated us to take up the challenge of this project. A prototype was designed and hand constructed with off the shelf available materials and hardware in the open market. The prototype was tested at the energy centre MANIT Bhopal, and the natural frequency of oscillation of each cylinder, the damping ratios, and the hydrodynamic mass of the cylinders were measured. Further testing of the prototype was conducted in the wind tunnel to measure the



hydrodynamic properties like, displacement, velocity, and acceleration of the cylinder at various wind velocities.

2.0.Principle of Vortex Induced Vibrations (VIVs)

Vortex shedding is a physical phenomenon which occur far and wide in the nature and it applies to each and every non-streamlined body (bluff body) immersed in a flowing fluid. The pressure of the flowing fluid near the bluff body increases from the free stream pressure which is away from the body to the stagnation pressure which is near in front of the body. This leads to the formation of boundary layer on the surface of the bluff body due to the viscosity of the fluid for all the Reynolds number except too small of the flows. The outer fluid layers which are in touch of the free stream, are moving faster than the inner side layers which are in touch with the wake. After some point along the body's surface, flow will not be able to follow the surface boundary and the boundary fluid layers are separated from the body. The separation angle and distance from the body depend on its surface geometries. These separated fluid layers form the wake and free stream and this formation causes rotation of the fluid. Rotation of the fluid causes the formation of vortices (called Vortex Street or Karman Vortex Street) behind the body and due to asymmetrical pressure distribution on the lower and upper parts of the body these vortices are shed away near periodic fashion from the body travel along the wake. In this process and due to the periodic pressure differential, an alternating net lift force transverse to the direction of the fluid transverse to the flow direction is exerted on the body, making the body to oscillate at the frequency of vortex shedding. The formation of different types of Karman vortex streets depends on the physical properties of the fluid (e.g. viscosity) and the characteristics of the flow (e.g. flow velocity). This phenomenon is called vortex-induced vibrations (VIV). Appropriate power conversion mechanisms can be utilized to harness this mechanical vibrational energy. This method is suitable for both air as well as water flow.

Another significant phenomena that is similar to linear resonance and is known as "lock in" or "synchronisation" can happen when the vortex shedding frequency (f_s) gets closer to the body's natural oscillation frequency (f_n) in fluid. This causes the non-linear resonance of the body's oscillation, which in turn increases the amplitudes of vibration. Since the process of vortex shedding and vibrations of the bluff body, affect each other by feedback loops created by fluid structure interaction so it does not produce the amplitude spikes at exactly the natural frequency. As the amplitude of vibration increases, the vortex shedding is weakened, making the further motion of the bluff body to slow down. Therefore, the lock-in is characterised as both a self-limiting and self-governing phenomenon. For VIV the laminar flow is preferred because it creates a broader wake pattern downstream of the cylinder, so the vortex shedding magnitude obtained is maximum, which results in larger lift force on the cylinder.



In the design of VIV energyharvester, for lock-in to occur, the range of frequencies of vortex shedding, f_{st} should matches to body's natural frequency of oscillation, f_n :

$$f_n = \frac{1}{2\pi} \sqrt{\left(\frac{k_{eq}}{m_{app}}\right)} \quad (2.1)$$

Where k_{eq} is the equivalent stiffness of suspension (spring) and m_{app} is applied mass to the bluff body (cylinder).

For parallel connection of springs: $k_{eq} = k_1 + k_2$

$$(2.2)$$

While for series connection of springs: $\frac{1}{k_{eq}} = \frac{1}{k_1} + \frac{1}{k_2}$

$$(2.3)$$

2.1. Reynolds Number (Re)

The ratio of inertial forces to viscous forces on the bluffbody within the moving stream is known as Re. Depending on its flow pattern is characterized as laminar ($Re < 1 \times 10^5$), transitional ($1 \times 10^5 < Re < 5 \times 10^5$), or turbulent ($Re > 5 \times 10^5$) flow. The pattern of VIV vortex shedding is affected by Re number. The Re number is given as [1]:

$$Re = \frac{UD}{\nu} = \frac{\rho UD}{\mu} \quad (2.4)$$

Where ν is the fluid's kinematic viscosity, ρ is the fluid's density, and μ is the viscosity of the fluid. U is the free-stream velocity. D is the cylinder's diameter.

2.2. Strouhal Number (St)

The Strouhal number, a non-dimensional quantity, connects the oscillating flow mechanism to the frequency of vortex shedding, f_{st} [1]. It is expressed as: $S_t = f_{st} D/U$

$$(2.5)$$

For Reynolds number ranging in between 1×10^4 to 7×10^4 , the Strouhal number can approximated to (Resvanis, MIT): $S_t(U) = -0.0065 \times \ln(R_e(U)) + 0.21$ (2.6)

Further, it can also be found by another empirical relation as: $S_t = 1.98 \left[1 - \left(\frac{19.7}{Re}\right)\right]$

$$(2.7)$$

3.0. Selected Design and Experimental Set Up

In its simplest form, a VIVEC (vortex induced based energy converter) module consists of a hollow cylinder (bluff body) suspended from springs and connected to a power take-off



(power converter) system with the help of a transmission mechanism for electricity generation.

We have chosen four cylinders of equal length (50 cm) and different diameters (2.54 cm, 5.08 cm, 7.62 cm, and 10.16 cm) as the aerofoil for VIVWPGEN so the performance of the devices depending on length to diameter ratio can be assessed. We have chosen a cylinder as aerofoil because it is able to harness lift force equally in both directions (up and down) of the oscillation. Our designed device consists of a cylinder suspended from by four springs at equilibrium, two springs are connected at one end of the cylinder along the center of cross-section of the cylinder and other two springs at the another end of the cylinder. Two additional support rods run through the cylinder and the springs along its midline. These support rods used are of lesser diameter than inner diameter of the springs and the holes in the cylinder through which they run, to avoid any drag force due to contact with cylinder or springs, however contact could be made producing friction if excessive drag force causes cylinder to deviate from its path of vertical oscillation; in that case, rods are meant to act as guide rails for the device and keep it from moving or twisting under the excessive drag force. One rod is attached to the cylinder, to which other end is attached a small hammer. This rod moves up and down as the cylinder makes oscillation and the hammer connected to its one end, and away from cylinder applies periodic compressive force on the piezoelectric, producing electricity.

Also a wire coil assembly is attached at both end of the cylinder extending outward. These coils act as electromagnet which moves back and forth within other coils, acting as a stator of the linear electric generator through which electricity produced is fetched. This arrangement could be reversed as instead of using electromagnet, a hollow cylindrical permanent magnet is used and the coils attached with cylinder moves within it. The coils are fixed on the walls of the foundation structure and the piezoelectric are fixed on the top of the foundation structure, as shown in the **Figure 3.1**.

4.0. Model Calculations

A simplified mathematical model is developed to predict the parameters of oscillating cylinder and to describe the oscillator dynamics of oscillator and fluid interaction so as to estimate the possible dynamic performance of a VIV system. Values used in these calculations were either taken from literatures or chosen by the experiments performed. The length and diameter were chosen on the basis of materials availability and space limitations of the wind tunnel.

Table 4.1: Cylinder properties and parameters.

$Crosssectionalareaofthecylinder(A_{cyl}) = Length(L) \times Diameter (D)$	The vortex shedding frequency: $f_{st} =$
--	---



(4.1)	$[S_t U/D]$ (4.6)
	For a wind velocity of 5 m/s, it is calculated to be: 13 cycles/s.
$Added\ mass = m_{add} =$ $mass\ of\ all\ appendages + \frac{1}{3} mass\ of\ spring$ (4.2)	$Total\ oscillating\ mass =$ $total\ applied\ mass\ to\ the\ system =$ $m_{app} = m_{osc} = m_{pipe} + m_{dis}$ (4.7)
$Mass\ of\ cylinder = m_{cyl} = \rho_{cyl} \times L +$ m_{add} (4.3)	Spring stiffness, $k = (2\pi f_n)^2 \cdot m_{app}$ (4.8) (Assume $f_n = f_{st}$)
$Volume\ of\ displaced\ fluid = m_{dis} = \frac{\pi}{4} D^2 L$ (4.4)	The drag force on the cylinder: $F_D =$ $0.5 \rho_{air} U^2 D L C_D$ (4.9)
$Mass\ of\ displaced\ fluid = m_{dis} =$ $\rho_{fluid} \times volume\ of\ cylinder$ (4.5)	The lift force on the cylinder: $F_L =$ $0.5 \rho_{air} U^2 D L C_L$ (4.10)
Density of the air $\rho_{air} = 1.225\ kg/m^3$ and C_L is the coefficient of lift and C_D is the drag coefficient over the cylinder (equal to 1: in this case based on the Re and geometry). The mass of the cylinder is calculated by using a researched weight to length ratio (density) of PVC piping, taken from the Engineering Tool Box.	

Table 4.2: Oscillation properties.

The variable lift force with respect to fluid velocity and time: $F_L(t, U) = F_L(U) * \sin(2\pi f(U)t)$; (4.11)

Where $F_L(U)$ is the lift force, U is the variable wind velocity, $f(U)$ is vortex shedding frequency depending on U , and t is the time. (For a smooth cylinder in cross flow, both the lift and drag coefficients are equal to 1.

Then, the velocity of the cylinder: $v(t) = \frac{Displacement}{Time\ taken}$
 (4.12)

Power extracted by VIVEC is: $P(t) = v(t) \times F_L(U) \sin(\omega t)$;
 (4.13)

The power $P(t)$, frequency is double the frequency of lift force or velocity of the



cylinder because it has two sine terms multiplied together.	
Mean power extracted by cylinder	is: $P_{rms} = P_{max}/\sqrt{2}$
(4.14)	
The theoretical maximum power available in the fluid is: $P_{fluid} = 0.5\rho_{fluid}U^3DL$	
(4.15)	
Efficiency of the <u>VIVEC</u>	is: $\eta = P_{rms}/P_{fluid}$
(4.16)	



Figure 3.1: Experimental set up (prototype model) of VIVWPGEN with foundation structure.

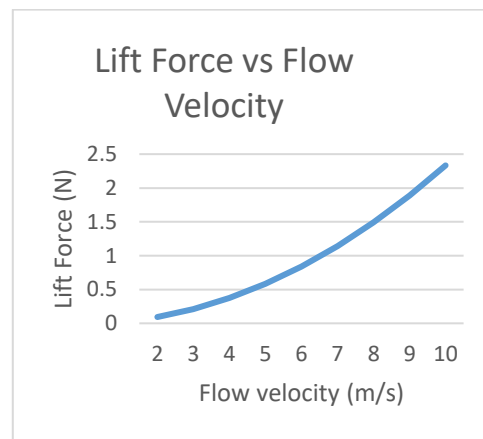


Figure 4.2: Lift Force (N) versus Flow Velocity (m/s).

Further the amplitude of the oscillation required to be calculated in order to find out the displacement of the coil. This is obtained by combining the following equations: $F_L(U) = m_{cyl} * a_{max}$ (4.17)

Where a_{max} is the maximum acceleration of the cylinder, given by: $a_{max} = (2\pi f(U))^2 * A$ (4.18)

Now the amplitude (A) can be found by solving for the maximum acceleration, as: $A(U) = \frac{F_L(U)}{(m_{cyl} * (2\pi f(U))^2)}$ (4.19)

According to Faraday's law of electromagnetic induction, voltage or electromotive force (emf) is produced as the coil moves in relation to the magnet since the coil's magnetic flux also changes.



The induced emf is: $\epsilon = -N \frac{\Delta\phi_B}{\Delta t}$

(4.20)

Where, the induced electromotive force (emf) is represented by ϵ , the magnetic flux change is represented by $\Delta\phi_B$, which is equal to $\Delta(B * A_c)$, and the magnetic field is represented by B , which is set to be between 0 and 1.5 T.

$A_c = \text{cross sectional area of the coil} = \pi r^2$ ($r = 0.9$ cm, chosen)

(4.21)

Rate of change in magnetic flux is calculated by using change in time that the cylinder takes to reach the maximum displacement (amplitude) from its equilibrium position. This change in time is equal to one quarter of the cylinder's period of oscillation. Further this is the amount of time, taken by the magnet to fully enter into the coil or to be pulled out from the coil, and is given as: $\Delta t = \frac{1}{4f(U)}$

(4.22)

Since the cylinder's oscillation is sinusoidal therefore voltage generated is also sinusoidal means AC voltage is generated. The AC voltage generated can be plotted for a specific wind velocity (5 m/s) with the following equation:

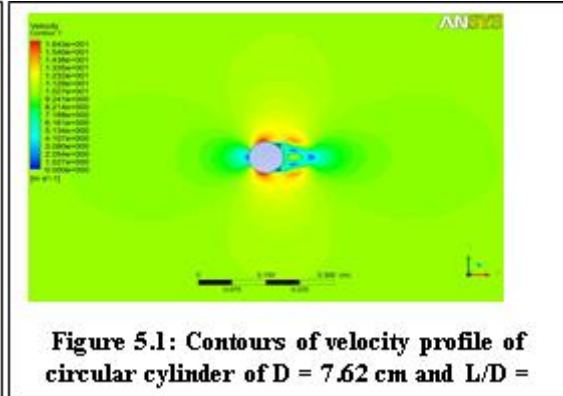
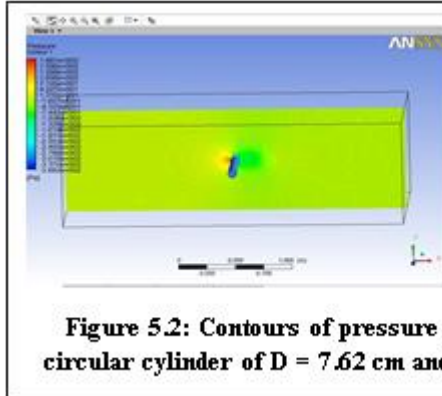
AC voltage, $V(t, U) = \epsilon(U) * \sin(2\pi f(U)t)$

S(4.23)

The diameter of the coils and magnetic field (B), we chosen are limited by available space, the maximum lift force produced and materials. The number of turns in the coils can be increased to increase the voltage generated.

5.0. Results and Discussion

We did the initial model calculation of VIVWPGEN for wind energy conversion and compared the theoretical results with the experimental results obtained. The range of Re Number taken in these calculation is ($300 < \text{Re} < 3 \times 10^5$) and this range falls in fully turbulent vortex regime, and for this range the Strouhal number is calculated about 0.2 for smooth surface body. All the simulations were performed in Ansys Fluent V-14.0. The fine mesh was generated, and double precision, transient analysis were performed. The results of velocity contours obtained clearly show the Van Karman's effect in the wake. The coefficient of drag profiles obtained clearly show that it is fluctuating initially and then go to initialise at some particular value. The coefficients of drag obtained are different for different geometries chosen. It is maximum for rectangular geometry. The coefficient of lift profiles obtained clearly show that it is zero initially and after some time it starts fluctuation and as the time elapses it is oscillating between some positive and negative values. The coefficients of lift obtained are different for different geometries chosen. For rectangular geometry the



coefficient of drag obtained is more than the coefficient of lift. And this is also true for the hexagonal geometry. Nonetheless, the coefficient of drag force and the coefficient of lift force are nearly equivalent for cylindrical geometries. For cylindrical geometries, these coefficient of lift force and coefficient of drag force values are in agreement with theory, as was discussed in chapter 3 and chapter 5. Therefore we went to choose the cylindrical geometries for our project prototype. And further we did our initial model calculations for cylindrical geometries of different length to diameter (L/D) ratios. We went to simulate and analyse the four different cylinders of diameters of 50.8 mm, 76.2 mm, 101.6 mm, and 127 mm respectively in order to access the effect of L/D ratios on the performance, the power generated and the efficiency of the VIVWGEN system.

We investigated the flow parameters of the cylinder which are listed in Table 5.1. Based on the initial model calculation obtained, the theoretical results are presented below in Table 5.2 and Table 5.3. To achieve the lock in, the suitable value of spring constants, k of springs for each testing cylinder is chosen based on diameter of cylinder to match the vortex shedding frequency with natural frequency of cylinder. It is evident from table 5.2 that value of spring constant, k decreases with the increase of cylinder's diameter. The difference in k value of springs are due to the difference in applied mass of the system for different cylinders.

Table 5.1: Description of dimensional and dimensionless variables.						
Cylinder and Flow Parameters					Air Properties	
Diameter, D (m)	0.025 4	0.050 8	0.076 2	0.101 6	Velocity, U (m/s)	3, 4 and 5
Length, L (m)	0.5	0.5	0.5	0.5	(4 m/s average air velocity in Bhopal)	
Length to Diameter (L/D)	19.69	9.84	6.56	4.92	Air Density (kg/m ³)	1.225



ratio						
Volume (m ³)	0.0003	0.001	0.0023	0.0041	Viscosity of Air (m ² /s)	1.7894 x10 ⁽⁻⁵⁾
Wall Thickness (cm)	0.338	0.391	0.549	0.602	Kinematic Viscosity of Air (m ² /s)	1.468* 10 ⁽⁻⁵⁾
Density (kg/m ³)	0.476	1.01	2.09	2.99		
Mass (kg)	0.238	0.505	1.045	1.495		
Mass of displaced air Mdisp (kg)	0.0003	0.0012	0.0028	0.0050		
Applied mass on Cylinder Mapp (kg)	0.2383	0.5062	1.0478	1.4999		

From Table 5.2 and Table 5.3, it is evident, increase in the diameter of the cylinder while other parameters are kept constant, increases in general, the Reynolds number Re , which results in larger amplitude of oscillation of the cylinder. It is also clearly evident that the maximum harness-able power in the system increases with the increase in Re number which is directly proportional to the diameter of cylinder. Since velocity of the cylinder increase with Re number which results, increased rate of power generation. The maximum efficiency in this experiment is obtained for the cylinder of 0.1016 m diameter. It is evident that power efficiency of the system increases with diameter of the cylinder. Also efficiency of the power production is affected by the fluctuation in motion of cylinder due to random behaviour of the vortex shedding.

We modified the design by removing the guide rods and using cylinder of a lighter weight PVC material to reduce the applied mass on the system thereby reducing the friction. Due to these changes in the design, the cylinder was able to make oscillation. We recorded the values and compared them with the calculated results as presented in the Table 5.4. The calculated amplitudes were much smaller than the actual measured amplitudes. The predicated values of amplitudes are only representative of the amplitudes that the system could achieve in the condition of lock in.

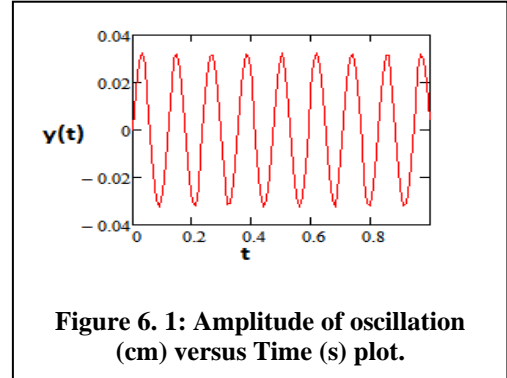
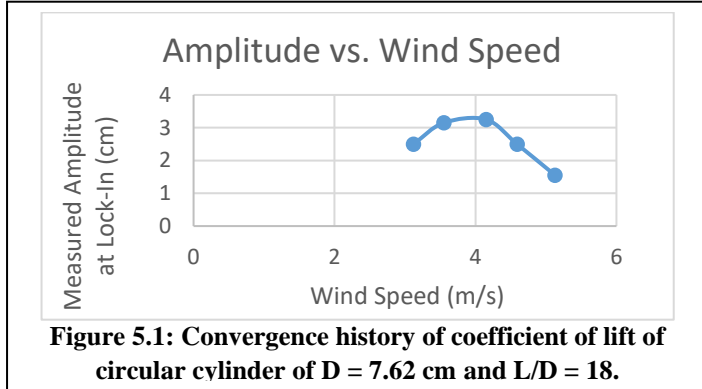


Table 5.2: Theoretical model calculations and results.

D (m)	U (m/s)	Re	$f_s = f_n$ (Hz)	K (N/m)	Fl (N)	y(t) max (m)	v(t) max (m/s)	P(t) max (W)	Prms (w)	P air (w)	η
0.0254	3	5217	23.3	5101	0.200	0.0003	0.048	0.010	0.007	0.210	0.032
0.0508	3	10433	11.7	2719	0.399	0.0012	0.090	0.036	0.025	0.420	0.060
0.0762	3	15650	7.8	2505	0.599	0.0020	0.097	0.058	0.041	0.630	0.065
0.1016	3	20866	5.8	2018	0.798	0.0033	0.121	0.096	0.068	0.840	0.081
0.0254	4	6955	31.1	9086	0.473	0.0004	0.085	0.040	0.028	0.498	0.057
0.0508	4	13911	15.6	4839	0.946	0.0016	0.159	0.151	0.107	0.996	0.107
0.0762	4	20866	10.4	4456	1.419	0.0027	0.173	0.246	0.174	1.494	0.116
0.1016	4	27822	7.8	3590	1.892	0.0044	0.215	0.406	0.287	1.991	0.144
0.0254	5	8694	38.9	14213	0.924	0.0005	0.132	0.122	0.086	0.972	0.089



0.0508	5	17389	19.5	7565	1.847	0.0020	0.249	0.460	0.325	1.945	0.167
0.0762	5	26083	13.0	6965	2.771	0.0033	0.270	0.749	0.530	2.917	0.182
0.1016	5	34777	9.7	5610	3.695	0.0055	0.336	1.240	0.877	3.889	0.226

Table 5.3: Experimental measurements and Theoretical model calculations and results.

D (m)	U (m/s)	Re	(fst = fn) (cycle/s)	Ma pp (kg)	K (N/m)	FD (N)	FL (N)	A (cm)	V(t) max (m/s)	P max (W)	Prms (w)	Pair (w)	η
0.0254	3.12	5425	24.233	0.2383	5519	0.076	0.076	0.0451	0.12	0.009	0.0064	0.236	0.0272
0.0508	3.12	10850	12.139	0.5062	2942	0.151	0.151	0.1692	0.225	0.034	0.0242	0.473	0.0511
0.0762	3.12	16276	8.0973	1.0478	2709	0.227	0.227	0.2755	0.244	0.056	0.0394	0.709	0.0556
0.1016	3.12	21701	6.0748	1.53	2183	0.303	0.303	0.4559	0.303	0.092	0.0652	0.945	0.069
0.0254	3.55	6173	27.585	0.2383	7152	0.098	0.098	0.0450	0.136	0.013	0.0095	0.348	0.0272
0.0508	3.55	12346	13.815	0.5062	3810	0.196	0.196	0.1691	0.256	0.05	0.0356	0.696	0.0511
0.0762	3.55	18519	9.2146	1.0478	3509	0.294	0.294	0.2754	0.278	0.082	0.058	1.044	0.0555
0.1016	3.55	24692	6.9128	1.57	2827	0.392	0.392	0.4558	0.345	0.135	0.096	1.392	0.069
0.0254	4.15	7216	32.262	0.2383	9782	0.134	0.134	0.0450	0.159	0.021	0.0151	0.556	0.0272



0.0508	4.15	14432	16.153	0.5062	5209	0.268	0.268	0.1690	0.299	0.08	0.0568	1.112	0.0511
0.0762	4.15	21649	10.774	1.0478	4796	0.402	0.402	0.2754	0.325	0.131	0.0926	1.668	0.0555
0.1016	4.15	28865	8.0821	1.5	3864	0.536	0.536	0.4557	0.404	0.216	0.1534	2.224	0.069
0.0254	4.59	7981	35.692	0.2383	11973	0.164	0.164	0.0450	0.176	0.029	0.0204	0.752	0.0272
0.0508	4.59	15963	17.868	0.5062	6374	0.328	0.328	0.1690	0.331	0.108	0.0769	1.504	0.0511
0.0762	4.59	23944	11.917	1.0478	5868	0.492	0.492	0.2753	0.359	0.177	0.1253	2.257	0.0555
0.1016	4.59	31925	8.9396	1.5	4728	0.656	0.656	0.4557	0.446	0.293	0.2075	3.009	0.069
0.0254	5.13	8920	39.901	0.2383	14964	0.205	0.205	0.0450	0.197	0.04	0.0285	1.05	0.0272
0.0508	5.13	17841	19.973	0.5062	7964	0.409	0.409	0.1689	0.37	0.151	0.1073	2.1	0.0511
0.0762	5.13	26761	13.32	1.0478	7332	0.614	0.614	0.2753	0.402	0.247	0.1749	3.151	0.0555
0.1016	5.13	35681	9.9919	1.5	5906	0.819	0.819	0.4556	0.499	0.408	0.2896	4.201	0.0689

In practice as the cylinder had achieved synchronisation, the amplitude goes on increasing until constrained by the forces applied by the springs. This condition was not taken into account in calculations, therefore showing the discrepancy in the calculated and experimental results. A graph between amplitudes and wind speed is shown in the Figure 5.1.

As evident from Table 5.4, calculated frequencies are of about the same order of magnitude as the measured frequencies, however they are almost linear. This is due to the reason that the springs (k values) should be adjusted as the air velocity was changing because change in air velocity changes the Re number, which in turn changes the applied mass on the cylinder, which in turn changes the spring constant. However due to practical limitations, springs could not be changed frequently, according to the flow velocity, therefore the actual data are limited



by the spring constant. This limitation makes the system complicated and imposes a limitation on its commercial implementation, unless until resolved by some innovative engineering solution. Further use of the same spring (k value) would make the system inefficient and it will work and produce electrical power only within a limited range of wind flow velocities, but this would simplify the system's complexities with sacrifice of little power. Experimentally measured frequencies of oscillation were generally are of the same order of magnitude of the theoretically calculated vortex shedding frequency. The amplitudes of oscillation measured were differed in few order of magnitude because of the differences in the added mass applied to the system

Table 5.4: Wind Tunnel Testing Data for cylinder of diameter 10.16 cm.

S. No.	Wind Speed (U) (m/s)	Calculated Amplitude (cm)	Lock-In Amplitude (cm)	Calculated Frequency (cycles/sec)	Measured Frequency (cycles/sec)
1.	3.12	0.4559	2.5	6.07	4.5
2.	3.55	0.4558	3.15	6.91	4.5
3.	4.15	0.4557	3.25	8.08	4.75
4.	4.59	0.4557	2.5	8.93	5.25
5.	5.13	0.4556	1.0	9.99	5.14

Maximum power produced is quite small due to smaller amplitude of cylinder oscillation attained. Therefore, a single unit of VIV power system is not enough to meet the power requirement of a physical household/commercial system. However, large number of VIV module installed in an array of units can generate enough power to meet the demand of a physical application. Also the VIV power system can be integrated with other renewable power system such as wind, solar to overcome the limitations of each other and to make a more sustainable renewable energy system.

6.0. Conclusions and Future Scope

Mass imposed a challenge when adding the power take off mechanism such as hammer to press piezoelectric, and the coils and magnet assembly to the system. The added mass was too much and therefore the small lift forces produced were not able to overcome the weight of the system to initiate the motion of the cylinder. Therefore we omitted the hammer and



piezoelectric power take off mechanism for future developments, and resorted to the coil, magnet assembly as the only power take off mechanism.

Furthermore, the cylinder motion could only be accomplished with small coils having less number of turns so of light weight. The voltage produced was too small, because of a small coil was used and use of larger coils to produce more voltage was restricted due to weight constraints.

We were not able to measure changes in oscillation behaviour of the cylinder below or above lock-in. The parameters obtained from test results were used in the differential equation of motion for the cylinders and the lift force with respect to time and the power transferred from the wind flow were calculated. However, because of inconsistencies between theoretical added mass and observed added mass and other observational limitations, this approach would predict only approximate outcomes.

Friction created due to support rods added initially as a guide mechanism to the cylinder was another important design constraint observed. Conceptually, the supports rods were added initially to the system to minimise the effects of drag force, instead, the drag force was created due to friction between the rods and the cylinder and system was dampened. Therefore we removed the guide rods we found that there was no any serious issue from the drag force. The slight horizontal movement of cylinder due to drag force was of not having any serious concern to the vertical motion of the cylinder, also in addition, we found no appreciable twisting about a vertical axis, what we incorrectly predicated. The conclusion of whole these exercise was that friction was a more serious problem than undesired horizontal motion of the cylinder, which actually was not occurring at the low wind velocities regime being tested. It was actually the friction which was dampening the system and forcing the cylinder from possible motion.

In future research, a more comprehensive list of bluff body's geometries and some degree of optimization of the shape of the bluff bodies should be tested. Another feature that could be researched in future is bluff body's surface roughness and its effect on the produced vortices and VIV induced motion.

REFERENCES

- [1] Fatin Alias, MohdAsamudin A. Rahman; "A bibliometric analysis on energy harvesting from vortex-induced vibration"; Cogent Engineering , Volume 11, 2024 - Issue 1.
- [2] Huang Haobo, Cao Di, Zhou Zhiyong, Du Wenfeng. Research progress of piezoelectric wind energy harvesters based on vortex-induced vibration. Chinese Journal of Theoretical and Applied Mechanics, 2023, 55(10): 2132-2145. doi: 10.6052/0459-1879-23-364



- [3] Magdy Roman, RowidaSobh, MomtazSedrak&Mohamed Ali; “Power performance enhancement of vortex-induced vibration wind turbines using a semi-active control approach”;
Energy Sources, Part A: Recovery, Utilization, and Environmental Effects; 21 Nov 2021, doi.org/10.1080/15567036.2021.2006830\
- [4] MayankVerma, Ashoke De; “Dynamics of vortex-induced-vibrations of a slit-offset circular cylinder for energy harvesting at low Reynolds number”; *Physics of Fluids* 34, 083607 (2022); <https://doi.org/10.1063/5.0103136>
- [5] Ratan Kumar Das, Muhammad TaharatGalib, “Design and Analysis of A Vortex Induced Vibration Based Oscillating Free Stream Energy Converter”; *Journal of Engineering Advancements*, June 2021 2(02):112-117
- [6] Dan Zhang, Rui Wang, BeichaoZheng “Vortex-Induced Vibration Analysis of Wind Turbine Flexible Tower”; *Advanced Manufacturing and Automation XII*; January 2023; *Lecture Notes in Electrical Engineering*; DOI: 10.1007/978-981-19-9338-1_62.
- [7] MuhammadHafizh,Asan, G.A. Muthalif , Jamil Renno , et.al.; “Vortex induced vibration energy harvesting using magnetically coupled broadband circular-array piezoelectric patch: Modelling, parametric study, and experiments”; *Energy Conversion and Management*; Volume 276, 15 January 2023, 116559.
- [8] Zhangyi Liao, AnpingXiong and Renxin Liu; “Study on Parameterization of Vortex-Induced Vibration Energy Harvester in Agricultural Environment”; *AgriEngineering* 2020, 2(4), 511-522.
- [9] M. A. Zahari, S. S. Dol; “Application of Vortex Induced Vibration Energy Generation Technologies to the Offshore Oil and Gas Platform: The Preliminary Study”; *World Academy of Science, Engineering and Technology, International Journal of Mechanical, Aerospace, Industrial, Mechatronic and Manufacturing Engineering* Vol: 8, No: 7, 2014, pp. 1321-1324.
- [10] M. M. Bernitsas, K. Raghavan, Y. Ben-Simon, and E. M. Garcia; “VIVACE (Vortex Induced Vibration Aquatic Clean Energy): A New Concept in Generation of Clean and Renewable Energy From Fluid Flow”; *Int. J. Offshore Mechanics and Arctic Engineering*, 2006, pp. 1-15.
- [11] A. Hall-Stinson, C. Lehrman, and E. Tripp; “Energy Generation from Vortex Induced Vibration”; Thesis (B.S.); Worcester Polytechnic Institute, United States, 2011.
- [12] M Zahari, H B Chan, T H Yong and S Doll; “The Effects of Spring Stiffness on Vortex-Induced Vibration for Energy Generation”; *IOP Conf. Series: Materials Science and Engineering* 78 (2015).
- [13] M. A. Zahari, S. S. Dol; “Effect of Different Sizes of Cylinder Diameter on Vortex Induced Vibration Energy Generation”; *Journal of Applies Sciences* 15(5); 2015, pp. 783-791.



- [14] A. Vinod, A. Kashyap, A. Banerjee, and J. Kimball, “Augmenting Energy extraction From Vortex Induced Vibration Using Strips of Roughness/Thickness Combinations,” *Int. J. Marine Energy technology Symposium*, 2013.
- [15] I. Ball, T. Killen, S. Sakhuja, and E. Warner, *Energy Generation From Vortex Induced Vibration*, Thesis (B.S.), Worcester Polytechnic Institute, United States, 2012.
- [16] R.D. Gabbai, H. Benaroya; “An overview of modelling and experiments of vortex-induced vibration of circular cylinders”; *Science Direct, Journal of Sound and Vibration* 282 (2005) pp.-575–616.
- [17] Williamson, C. H. K., and Govardhan, R., 2004, “Vortex Induced Vibrations,” *Annu. Rev. Fluid Mech.*, 36, pp. 413–455.
- [18] Jauvtis, N., and Williamson, C. H. K., 2003, “Vortex-Induced Vibration of a Cylinder in Two Degrees of Freedom,” *J. Fluids Struct.* 17, pp. 1035–1048.
- [19] Sarpkaya, T., 2004, “A Critical Review of the Intrinsic Nature of Vortex Induced Vibrations,” *J. Fluids Struct.* 19_4_, pp. 389–447.
- [20] Bernitsas, M. M., Ben-Simon, Y., Raghavan, K., and Garcia, E. M. H., 2006, “The VIVACE Converter: Model Tests at High Damping and Reynolds Number Around 105,” *25th International OMAE Conference, San Diego, CA, 10–15 June 2007*.
- [21] Robert Correa, Eric Cremer, William Sweeney, Sarah Thomson (2014); “Wind Harvesting via Vortex Induced Vibration”; *Graduate dissertation; Worcester Polytechnic Institute, Massachusetts, USA*.
- [22] A. Techet, *Vortex Induced Vibration*. MIT Open Course Ware, Massachusetts Institute of Technology, United States, 2005.
- [23] R. D. Blevins, *Flow Induced vibration*, Thesis (Ph.D.), California Institute of Technology, California, 1974.